



Aalborg Universitet

AALBORG UNIVERSITY  
DENMARK

## Biocompatibility of the TIME Implantable Nerve Electrode

Badia, Jordi; Kundu, Aritra; Harreby, Kristian Rauhe; Boretius, Tim; Stieglitz, Thomas; Jensen, Winnie; Navarro, Xavier

*Published in:*

Direct Nerve Stimulation for Induction of Sensation and Treatment of Phantom Limb Pain

*Creative Commons License*  
CC BY-NC 4.0

*Publication date:*  
2019

*Document Version*  
Publisher's PDF, also known as Version of record

[Link to publication from Aalborg University](#)

*Citation for published version (APA):*

Badia, J., Kundu, A., Harreby, K. R., Boretius, T., Stieglitz, T., Jensen, W., & Navarro, X. (2019). Biocompatibility of the TIME Implantable Nerve Electrode. In *Direct Nerve Stimulation for Induction of Sensation and Treatment of Phantom Limb Pain* (pp. 155-169). River Publishers.

### General rights

Copyright and moral rights for the publications made accessible in the public portal are retained by the authors and/or other copyright owners and it is a condition of accessing publications that users recognise and abide by the legal requirements associated with these rights.

- Users may download and print one copy of any publication from the public portal for the purpose of private study or research.
- You may not further distribute the material or use it for any profit-making activity or commercial gain
- You may freely distribute the URL identifying the publication in the public portal -

### Take down policy

If you believe that this document breaches copyright please contact us at [vbn@aub.aau.dk](mailto:vbn@aub.aau.dk) providing details, and we will remove access to the work immediately and investigate your claim.

# 5

---

## Biocompatibility of the TIME Implantable Nerve Electrode

---

**Jordi Badia<sup>1,2</sup>, Aritra Kundu<sup>3</sup>, Kristian R. Harreby<sup>3</sup>, Tim Boretius<sup>4,5</sup>,  
Thomas Stieglitz<sup>5,6,7</sup>, Winnie Jensen<sup>3,\*</sup> and Xavier Navarro<sup>1,2,\*</sup>**

<sup>1</sup>Institute of Neurosciences and Department of Cell Biology, Physiology and Immunology, Universitat Autònoma de Barcelona, Bellaterra, Spain

<sup>2</sup>Centro de Investigación Biomédica en Red sobre Enfermedades Neurodegenerativas (CIBERNED), Spain

<sup>3</sup>Department of Health Science and Technology, Aalborg University, Denmark

<sup>4</sup>Neuroloop GmbH, Freiburg, Germany

<sup>5</sup>Laboratory for Biomedical Microsystems, Department of Microsystems Engineering-IMTEK, Albert-Ludwig-University of Freiburg, Freiburg, Germany

<sup>6</sup>BrainLinks-BrainTools, Albert-Ludwig-University of Freiburg, Freiburg, Germany

<sup>7</sup>Bernstein Center Freiburg, Albert-Ludwig-University of Freiburg, Freiburg, Germany

E-mail: xavier.navarro@uab.cat

\*Corresponding Authors

### 5.1 Introduction

A key component for the clinical applicability of neuroprostheses is the neural electrode, intended to bidirectionally exchange information with the nervous system, thus allowing recording of nerve signals and stimulation of nerves and muscles over extended periods of time. A prerequisite for the application of nerve electrodes is that the implant must be biocompatible.

Biocompatibility can be defined as “the ability of a material to perform an appropriate host response in a specific application” (Williams, 1987). The compatibility between a technical and a biological system can be divided into *structural biocompatibility* and *surface biocompatibility* (Stieglitz, 2004). Structural biocompatibility refers to the adaptation of the artificial structure to the mechanical properties of the surrounding tissue, so that the device design and material properties should adapt to the biological structure of the target tissue. Surface biocompatibility deals with the interaction of chemical, physical, and biological properties of the foreign material and the target tissue. A material can be considered biocompatible if substances are only released in nontoxic concentrations and the biological environment reacts only with a mild foreign body reaction and encapsulation with connective tissue. The design and size, as well as the material choice and the interface surface, have to ensure stable properties of the electrode-electrolyte interface throughout the implant lifetime (Navarro et al., 2005). Once implanted, a neural interface has to remain within the body of the subject for months or years, so the stability of the materials in the electrode is crucial. The electrode has to be resistant to corrosion during stimulation and to the attack of biological fluids, enzymes, and macrophages produced during the initial foreign body reaction. It must be composed of inert materials, both passively and when subjected to electrical stimulation, since deterioration of the device may result in implant failure and the release of toxic products.

The first step to determine if any electrode material is biocompatible is, on one side, the *in vitro* study, bringing cell cultures in contact with the material and evaluating different parameters as morphological and ultrastructural changes (Koeneman et al., 2004; Vince et al., 2004), and, on another side, the *in vivo* subcutaneous implant of the material to investigate the tissue reaction, evaluating the thickness of cellular layers that surround the material and the presence of inflammatory cells (Vince et al., 2004). The following step is the evaluation of the full electrode device implanted in the target tissue, in this case the peripheral nerve, chronically, assessing possible functional changes and structural damage to the nerve as a consequence of the implanted device.

The transverse intrafascicular multichannel electrode (TIME) (Boretius et al., 2010) is intended to be implanted transversally in the peripheral nerve and address several subgroups of nerve fibers with a single device. Therefore, in an initial stage of the TIME project we performed extensive *in vivo* studies in order to assess the biocompatibility and safety of TIMEs after implantation in the rat and the pig.

## 5.2 Biocompatibility of the TIME in the Rat Nerve Model

### 5.2.1 Biocompatibility of the Substrate and Components

Following the standards defined in the ISO-10993 protocol for testing local effects after implantation of a device, pieces of polyimide substrate containing deposited iridium oxide (IrOx) as conductor for the active sites of the device were implanted in the subcutaneous tissue of adult rats during 4 weeks. The hexagonal pieces of polyimide substrate, with a surface of 100 mm<sup>2</sup>, containing 19 deposited circles of IrOx (occupying a total of 50 mm<sup>2</sup>) were provided by IMTEK. After shaving and disinfecting the rat skin, four incisions 1.5 cm long were done bilaterally on the back of the animals, with a distance of 2.5 cm between incisions. Sterile pieces of polyimide or of silicone as control, were implanted subcutaneously, one in each prepared subcutaneous pocket. The incisions were then sutured and disinfected. After 4 weeks, animals were sacrificed, and perfused transcardially with 4% paraformaldehyde. The implanted specimens were removed with the surrounding skin tissue and processed for histological and immunohistochemical analyses.

Compared to the intact skin, samples that had the polyimide implant, as well as silicone sheath implant as control, showed the epidermis and the connective tissue layer, with normal organization and appearance, as revealed by hematoxylin-eosin staining (Figure 5.1).

There were not areas of necrotic tissue in the subcutaneous and muscle layers. However, both silicone and polyimide implants were surrounded by a dense thin capsule of connective tissue. The thickness of the fibrous capsule was larger in silicone sections (outer zone: 159 ± 35 μm; inner zone: 69 ± 21 μm) than in polyimide sections (outer zone: 107 ± 9 μm; inner zone: 60 ± 7 μm). Immunohistochemical labeling was used to assess the inflammatory reaction by estimating the presence of macrophages stained with Iba-1 antibody in the capsule surrounding the implants. In samples with silicone implants macrophages were present at the inner zone, near blood vessels, but not at the outer and lateral zones. Sections with polyimide implants showed also concentration of macrophages in the inner zone, and lower amount at lateral zones.

Polyimide-based materials have been demonstrated biocompatible with respect to toxicity (Richardson et al., 1993; Rihová, 1996) as well as to biostable in other types of electrodes implanted in vivo (Rodríguez et al., 2000; Ceballos et al., 2003; Lago et al., 2007). The histological biocompatibility assessment of the tissue surrounding the implants of polyimide

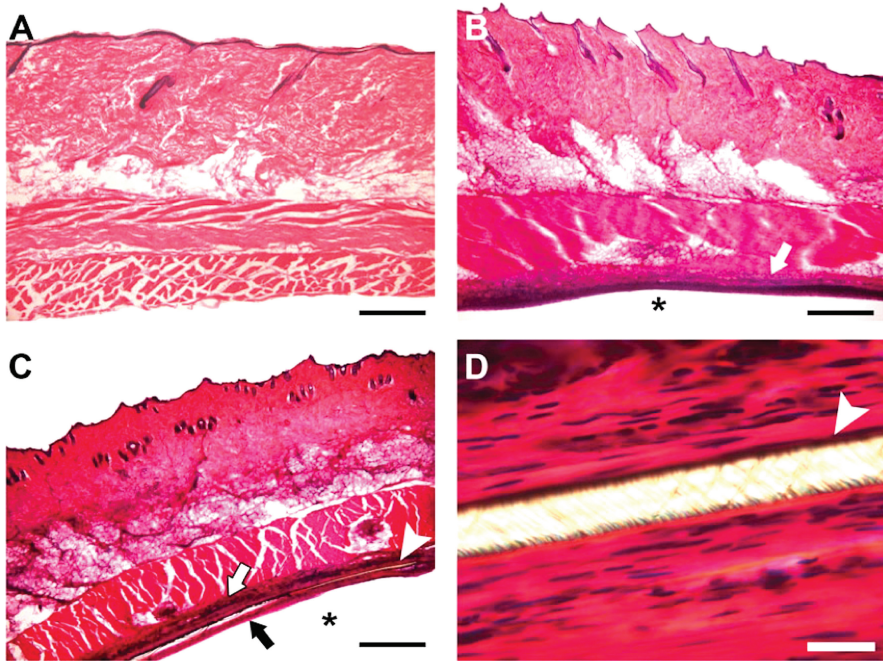


**Figure 5.1** Hematoxylin-eosin staining of representative sections from skin without implant (A), with a silicone implant (B) and with a polyimide implant ((C), and detail in (D)). (B) Silicone implants showed a cavity formed during tissue processing (asterisk). White arrows show the superficial fibrous layer (outer zone). (C) Polyimide implants were embedded in the fibrous capsule (white arrowheads). The deep fibrous layers of the capsule are also shown (inner zone, black arrow). Scale bars: 500  $\mu\text{m}$  ((A)–(C)) and 20  $\mu\text{m}$  (D).

containing IrOx dots, selected to fabricate the TIME, indicated good integration in the skin and subcutaneous tissue of the adult rat. This is in agreement with previous studies, describing the absence of a gross response to metal-coated pieces of polyimide or uncoated control silicone (Cogan et al., 2003). Although the capsule surrounding the implant was observed around both the unprocessed silicone and the metalized polyimide samples, it was significantly thinner in the latter. Macrophages were slightly more abundant next to polyimide than to silicone samples, but still their density was low, suggesting a slight degree of inflammatory response around the implanted materials.

### 5.2.2 Biocompatibility of the TIME Implanted in the Rat Nerve

The electrodes used in the study corresponded to the TIME-2 and TIME-3 designs, explained in the previous chapter, and were produced by the Department of Microsystems Engineering (IMTEK) of the University of Freiburg. Cleaned and sterilized TIMEs were implanted into the sciatic nerve of adult rats. In one group (Acute,  $n = 7$ ) of rats the TIME-2 was implanted and, in order to evaluate the damage just induced by the surgical implantation procedure, the electrode was retired after an acute electrical stimulation protocol was performed. In two other groups (TIME-2 and TIME-3,  $n = 5$  each) a TIME-2 or a TIME-3 were transversally implanted in the sciatic nerve and remained for 2 months.

The TIME devices were transversally inserted across the three fascicles of the sciatic nerve (sural, tibial, and peroneal branches) at the midthigh. The electrode was inserted with the help of a small straight needle attached to a 10-0 loop thread that was passed between the two arms of the TIME. The needle was inserted transversally across the sciatic nerve and then pulled the thin-film structure through it. Once the structure was implanted, the needle was removed by cutting the suture. The TIME-2 ribbon was routed across the overlying muscular plane to the lateral thigh region, where the ending part was secured under the skin. For the TIME-3 design, the ribbon was routed along the nerve and the ending pad was accommodated under the muscle (Figure 5.2).

All the animals were followed up with a battery of neurophysiological tests to obtain evidence of possible functional alterations, and final histological analysis to assess potential damage induced by the implanted TIMEs on the nerve. The study design aimed to discriminate effects due to the implantation procedure, to the presence of the intraneural electrode segment, and to the mechanical motion induced by the TIME ribbon and connector during chronic implants (Badia et al., 2011).

During the 2 months implantation time, there were no remarkable changes in any of the parameters of motor and sensory nerve conduction tests performed in any of the implanted groups, Acute, TIME-2, and TIME-3. The amplitude of the compound action potentials (CMAPs and CNAPs) obtained by stimulation of the right sciatic nerve after TIME-2 and TIME-3 implantation did not change notably at any interval postimplantation in comparison with the control nerve values. There was evidence of slight slowing of nerve conduction velocity at 7 days in the implanted groups, but it was normalized

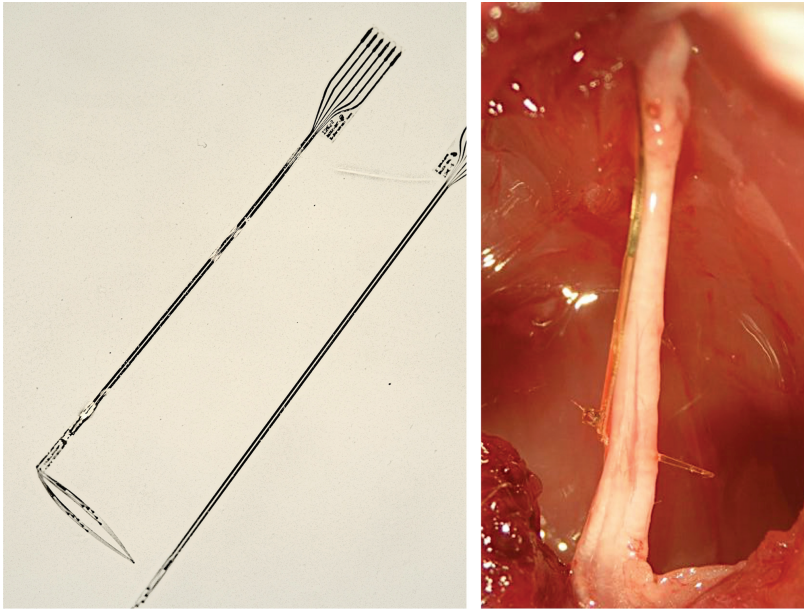


**Figure 5.2** Left: Photograph of a TIME-3 in which the intraneural portion is angled at 90°. Right: photograph of the insertion of a TIME-3 with the ribbon accommodated to the longitudinal axis of the sciatic nerve.

at 30 days. The implanted nerves showed similar values over time than the contralateral intact nerves (Figure 5.3A, B).

Walking track test, used to evaluate the locomotion performance, did not show variations between the right (TIME-2 and TIME-3 implanted) and left (intact) hindpaw prints along the follow-up. The Sciatic Functional Index averaged between  $-5$  and  $+20$  during follow-up (Figure 5.3C). The algometry tests yielded similar values of the pain threshold for withdrawal between the implanted and the contralateral sides, without evidence of hyperalgesia that might be induced by nerve compression or injury (Figure 5.3D). No loss of pain sensitivity was appreciated in any area of the hindpaw under pinprick testing.

### **5.2.3 Morphological Evaluation of the Implanted Nerves**

The macroscopic examination during final dissection at 2 months after implantation showed that the electrodes remained in place within the sciatic

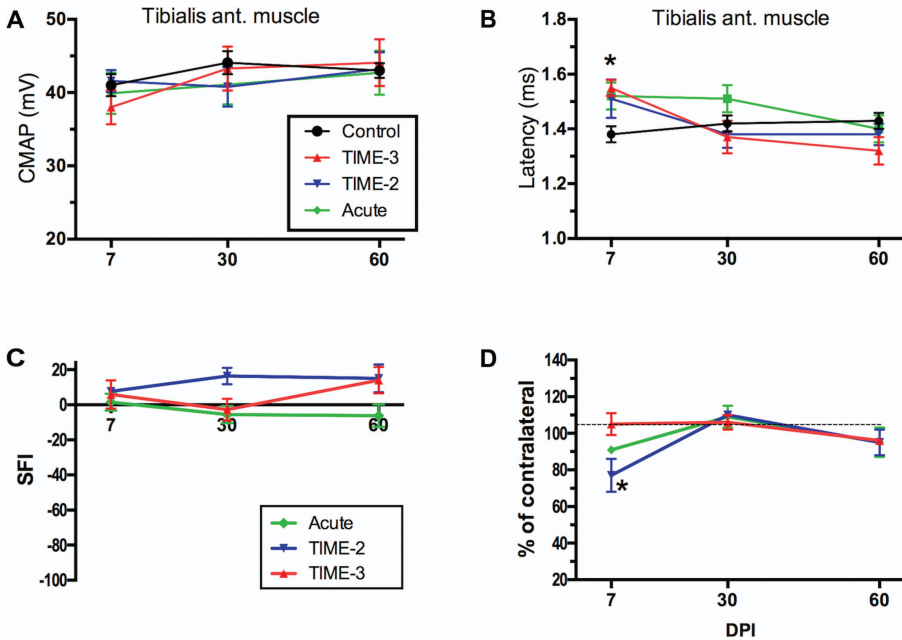


**Figure 5.3** Neurophysiological tests result in the three groups with Acute, TIME-2, and TIME-3 chronic implant in comparison with control values. Values of the CMAP amplitude (A) and onset latency (B) of the tibialis anterior muscle. Values of the SFI (C) and of algesimetry (D). Modified from Badia et al., 2011.

nerve in all animals of groups TIME-2 and TIME-3. Transverse sections at the segment that contained the intraneural TIME allowed to see the electrode strip crossing the fascicles of the sciatic nerve, covered by a fibrous tissue that disrupted the microarchitecture of the nerve (Figure 5.4).

Transverse semithin sections of the nerve distal to the insertion site showed a normal fascicular organization (Figure 5.4). The numbers of myelinated fibers counted in the distal level for each of the three branches of the sciatic nerve were in all the implanted groups similar to those found in control intact nerves. The reduction of about a 10% in the mean number of myelinated fibers of the sciatic nerve in group TIME-2 was mostly due to a decrease of myelinated fibers of about the 8% in the tibial nerve and 25% in the sural nerve, the smallest of the three branches. Group TIME-3 has only a small loss of myelinated fibers in the sural nerve (about 20%) (Badia et al., 2011).



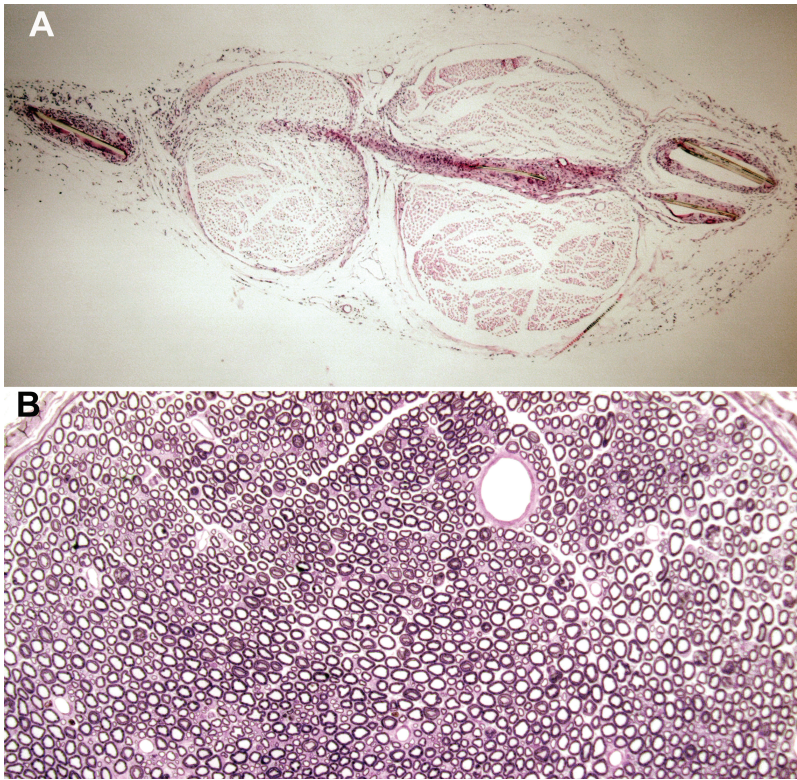


**Figure 5.4** Cross-sections of an implanted rat sciatic nerve. (A) At the level of TIME-3 implant crossing the tibial branch and part of the peroneal branch. Note the mild fibrous tissue surrounding the electrode. (B) Semithin transverse section of the tibial nerve of the same animal distal to the implant site. There are no signs of degeneration and the density of myelinated fibers is similar to controls.

### **5.3 Biocompatibility of the TIME in the Pig Nerve Model**

Device implantation and associated tissue injury trigger a cascade of inflammatory and wound healing responses that are typical of a foreign body response (FBR) (Morai et al., 2010). The continuous presence of biomaterial devices leads to chronic inflammation. The wound healing response depends on the size and extent of the implant. The end stage of FBR involves shielding the implant by a vascular and collagenous fibrous capsule (Williams et al., 1983; Labat-Robert, 1990; Kovacs et al., 1991). The response to any implant is wound healing comprised of hemostasis (seconds to hours), inflammation (hours to days), repair (days to weeks), and remodeling (weeks to months)

(Stroncek, 2008). To evaluate the biological effect of the TIME electrodes in the large nerve animal model (chronically implanted Göttingen minipigs), and particularly the fibrotic capsule formed around the electrode, we harvested and analyzed nerves following several weeks of implant.

All experimental procedures were approved by the Animal Experiments Inspectorate under the Danish Ministry of Justice. Female, Göttingen minipigs. Under full anesthesia and using aseptic surgical techniques one or two TIMEs were implanted in the median nerve above the elbow joint. If only one TIME electrode was implanted, it was placed at an angle of  $90^\circ$  or  $135^\circ$ . When two electrodes were implanted they were implanted with a  $45^\circ$  difference in angle. Lead-out wires were tunneled subcutaneously to the back of the pig where they exited the skin.

To collect tissue for histological evaluation an incision was made over the implant area and the location of the TIME and the median nerve were identified. The animal was then euthanized and the nerve including electrode(s) and lead-out wires was harvested. We performed further dissection of the harvested tissue in order to free the nerve and electrode from the surrounding fibrotic tissue (Figure 5.5). A specimen of approx. 5 mm of the nerve containing the TIME electrode was taken and either immersed in formalin or in liquid nitrogen. To maintain orientation of the nerve the proximal cross-section was marked with green dye while the entry and the exit point of the identified TIME electrodes were marked with blue. In one animal, we collected control samples from the right, nonimplanted leg. We included 11 animals in the study that were implanted during  $22 \pm 7.7$  days (range 8–37 days).

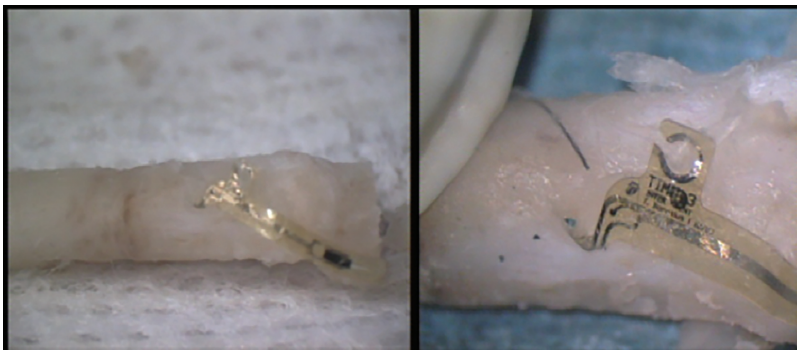


**Figure 5.5** Example of nerve specimen retrieved from a minipig after approx. 30 days of implant. The surrounding fibrotic tissue has been removed by careful dissection to identify the entry and exit points of the TIME.

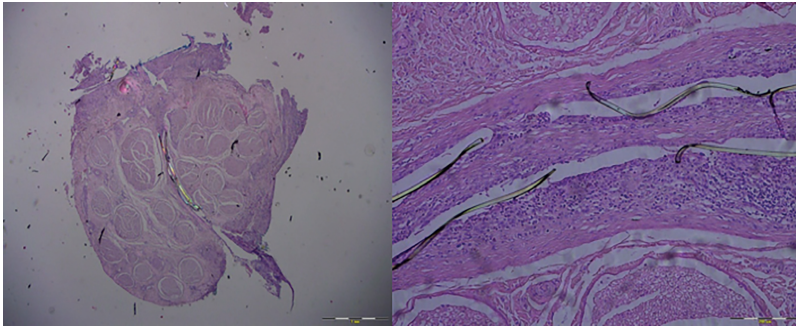


**Figure 5.6** Typical samples of H&E stains of the peripheral nerve, where the TIME electrode has been identified inside the nerve. Left ( $\times 20$ , Fig 02): whole nerve with TIME transverse through the nerve easily identified. Right ( $\times 100$ , Fig 02): higher magnification of the implant site – the TIME electrode and a layer of fibrosis surrounding the electrode is seen. The visible “cracks” inside the fascicles result from the processing and embedding the nerve.

Transverse sections of  $5\ \mu\text{m}$  thickness were cut in the nerve using a cryostat. The tissue was stained with Hematoxylin and Eosin (H&E) (Figure 5.6). To estimate the thickness of the fibrotic scarring, digital pictures were taken through a microscope. To avoid bias we randomly chose five points and measured the distance from the polyimide structure of the electrode to the rim of the fibrotic capsule perpendicularly.

### 5.3.1 Morphological Evaluation of the Implanted Nerves

All animals were in good health state and supported weight on the implanted leg. In approximately half of the animals we noticed signs of swelling, edema, and tenderness at the wound following the implant, which disappeared in the following 6–9 days. Eight of the 13 animals developed infection either at the implant wound or at the percutaneous connector in the back. In the majority of the cases we were able to treat the infection to a point where it was not possible to detect it visually.

*Layer of fibrosis.* Complete visualization of the entire length of TIMEs placed transversely through the nerves was not always possible. The estimated layer of fibrosis is shown in Table 5.1. The thickness of the fibrosis averaged  $108 \pm 40\ \mu\text{m}$ . A similar FBR was also identified in the histological evaluation of the rat sciatic nerve. We found no apparent correlation between the thickness of the fibrosis and the duration of the implant.

**Table 5.1** Estimated thickness of the fibrotic capsule formed around nine TIME electrodes implanted in seven pigs

Animal	Pig 01	Pig 02	Pig 04	Pig 06	Pig 09	Pig 10 TIME-1	Pig 10 TIME-2	Pig 11 TIME-1	Pig 11 TIME-2
Thickness [ $\mu\text{m}$ ]	74.3	62.0	179.6	71.4	128.3	116.4	141.6	117.9	100.4
Mean $\pm$ SD	$\pm 8.7$	$\pm 26.5$	$\pm 60.6$	$\pm 23.5$	$\pm 42.9$	$\pm 9.4$	$\pm 30.6$	$\pm 38.9$	$\pm 21.1$
# days implant	36	19	25	20	8	31	31	37	37

*Macroscopic changes.* For animals included in the “Chronic selectivity” experiments we found that typical inflammatory cells were present around the implant (i.e., including lymphocytes, macrophages, and giant cells), however some variation between animals was observed. Also we identified fibrocytes/fibroblasts in all animals. There were no signs of necrosis. The presence of inflammatory cells and fibroblasts/fibrocytes indicated that the wound healing process was likely still ongoing at the time of explant. It is important to note that the inflammatory response and the formation was only found around the electrode, i.e., the remaining part of the nerves and fascicles appeared normal and without presence of fibrosis or inflammatory response.

## 5.4 Discussion

Intraneural electrodes are intended to provide a good degree of sensitivity and selectivity for stimulation and recording action potentials at the nerve fibers of the implanted nerve fascicles. However, they have the risk of inducing damage to the nerve. Relative motion between the nerve and surrounding muscles during limb movement can exert forces on the electrode, and eventually extract it or damage the nerve if the electrode is unable to move with the nerve. Lead management and connector requirements offer additional challenges; lead wires or ribbon strips can produce tethering forces on the electrode, resulting in damage to the nerve or breakage of the device. The materials used for the TIME, i.e., polyimide as substrate and IrOx as conductive sites, are biocompatible, as corroborated in our study in subcutaneous implants. The induced FBR was similar or slightly thinner than with a control substrate as silicone.

In general, we found that all the animals implanted, either rats or pigs, showed good recovery from the surgery and were in good health during the implant period. The infections experienced are likely related to the pig model,

since no infections were observed in the rat model. However, the risk of infection in future human clinical experiments will be very low, since it is much easier to keep the percutaneous lead wires and exit points clean and protected.

From the surgical point of view, TIMEs were easy to implant in the nerve, because of the high flexibility and small thickness of the electrode strips, even in the small size nerves of the rat. The results of the follow-up evaluation indicate that either acute or chronic implantation of the TIME in the rat sciatic nerve for up to 2 months did not cause significant signs of axonopathy, axonal loss or demyelination, as evidenced by the functional and histological findings. Nerve conduction tests showed a mild increase in latency time at the first week after implantation, which is likely attributable to the surgical implantation procedure, since damage to the perineurium leads to endoneurial edema. Nevertheless, the degree of dysfunction was low and time limited, since the animals showed recovery toward normal values during the following weeks. Moreover, the nociceptive responses quantified by algometry tests showed a mild decrease of the threshold only at 7 days in the group TIME-2, whereas at 1 and 2 months there were no signs of hyperalgesia or pain. The absence of differences between the animals implanted with TIME-3 and their controls indicates that the tethering and motion forces, produced by the surrounding muscles and transmitted through the ribbon in the case of the TIME-2 implants, were minimized with the next TIME-3 design.

Regarding the histological results in the rat implanted nerves, the finding of a slightly reduced number of myelinated fibers distal to the implant site in group TIME-2 is suggestive of damage and subsequent axonal degeneration of a small population of nerve fibers. Nevertheless, we did not find images of ongoing degenerating fibers at 2 months, thus pointing to a time-limited damage, most likely occurring during insertion. Comparatively, the reduction of about a 10% in the number of myelinated nerve fibers with TIME-2 in the chronic group is similar to that previously reported after the implantation of other intrafascicular electrodes such as the polyimide thin film LIFE (Lago et al., 2007), which is coherent with the fact that the Young's modulus of the substrate material (polyimide, UBE U-Varnish-S) is similar between TIME and LIFE. The Utah Slanted Electrode Array (USEA) that is also inserted transversally to the nerve yielded results similar to the ones found for the TIME, although we did not find images of ongoing degenerative fibers at 2

months postimplant, in contrast with the results for the USEA (Branner et al., 2004); the difference may be attributed to the stiffness of the silicon USEA structure.

The reduction in the number of myelinated nerve fibers in the tibial nerve of the group TIME-2 was not observed in the group TIME-3. This difference can be explained because of the absence of traction forces with the TIME-3 design, this conclusion is reinforced by the fact that the nerves of the Acute group did not show fiber loss. The minor loss of myelinated fibers in group TIME-2 was not extensive enough to affect the animal function or electrophysiological responses. Since in group TIME-3 we did not find significant histological abnormalities, we can attribute most of the axonal loss in group TIME-2 to the effects produced by the traction forces for some days after implantation during the animal motion, and not to the material itself. The refinement in the geometrical design of the TIME-3 allows for a better adaptation of the structure to the anatomical properties of the nerve and to reduce the tethering forces to which the electrode may be subjected.

These conclusions were proved by the subsequent study of TIME-3 implants in the pig median nerve. There were no clinical evidences of nerve damage or dysfunction during several weeks of implant. The histological study of the harvested nerves did not show any appraten abnormality on the microstructure of the nerve, except for the presence of the transversal electrode, which was covered by a fibrous capsule, as corresponds to a normal FBR. The overall mean of the fibrosis was  $108 \pm 40 \mu\text{m}$ , which is comparable to what is found in the literature (Williams et al., 1983; Labat-Robert, 1990; Kovacs et al., 1991). A similar reaction and layer of fibrosis was also identified in the histological evaluation of the rat sciatic nerve. Interestingly, there was no apparent correlation between the thickness of the fibrotic scarring and the duration of the implant, thus suggesting that the FBR occurs during the first 1–2 weeks after implant, and thereafter remains stable, helping also to maintain the implanted electrode in place. The inflammatory response and fibrosis was only found around the electrode, i.e., the remaining part of the nerves appeared normal.

Altogether our results indicated that the TIMEs are biocompatible and safe after chronic implantation even in a small peripheral nerve, such as the rat sciatic nerve. The mild effects of the TIME on the nerve will be minimized when implanting the electrode of the same dimensions in larger nerves of humans.

## References

- Badia, J., Boretius, T., Pascual-Font, A., Udina, E., Stieglitz, T. and Navarro, X. (2011). Biocompatibility of chronically implanted transverse intrafascicular multichannel electrode (TIME) in the rat sciatic nerve. *IEEE Trans Biomed Eng* 58:2324–2332.
- Branner, A., Stein, R. B., Fernandez, E., Aoyagi, Y. and Normann, R. A. (2004). Long-term stimulation and recording with a penetrating microelectrode array in cat sciatic nerve. *IEEE Trans Biomed Eng* 51:146–157.
- Ceballos, D., Valero-Cabré, A., Valderrama, E., Schüttler, M., Stieglitz, T. and Navarro, X. (2002). Morphological and functional evaluation of peripheral nerve fibers regenerated through polyimide sieve electrodes over long term implantation. *J Biomed Mat Res* 60:517–528.
- Cogan, S. F., Edell, D. J., Guzelian, A. A., Liu, Y. P. and Edell, R. (2003). Plasma-enhanced chemical vapor deposited silicon carbide as an implantable dielectric coating. *J Biomed Mat Res* 67A:856–867.
- ISO 10993-6:2007 (E). International Standard. ‘Biological evaluation of medical devices. Part 6: Tests for local effects after implantation’, 2007.
- Koeneman, B. A., Lee, K. K., Singh, A., He, J., Raupp, G. B., Panitch, A. and Capco, D. G. (2004). An ex vivo method for evaluating the biocompatibility of neural electrodes in rat brain slice cultures. *J Neurosci Methods* 137:257–263.
- Kovacs, E. J. (1991). Fibrogenic cytokines: The role of immune mediators in the development of scar tissue. *Immunol Today* 12:17–23.
- Labat-Robert, J., Bihari-Varga, M. and Robert, L. (1990). Extracellular matrix. *FEBS Lett* 268:386–393.
- Lago, N., Yoshida, K., Koch, K. P. and Navarro, X. (2007). Assessment of biocompatibility of chronically implanted polyimide and platinum intrafascicular electrodes. *IEEE Trans Biomed Eng* 54:281–290.
- Morai, J., Papadimitrakopoulos, F. and Burgess, D. J. (2010). Biomaterials/tissue interactions: Possible solutions to overcome foreign body response. *Am Assoc Pharmaceut Scien J* 12:188–196.
- Navarro, X., Krueger, T., Lago, N., Micera, S., Stieglitz, T. and Dario, P. (2005). A critical review of interfaces with the peripheral nervous system for the control of neuroprostheses and hybrid bionic systems. *J Peripher Nerv System* 10:229–258.

- Richardson, R. R., Miller, J. A. and Reichert, W. M. (1993). Polyimides as biomaterials: Preliminary biocompatibility testing. *Biomaterials* 14:627–635.
- Rihová, B. (1996). Biocompatibility of biomaterials: Hemocompatibility, immunocompatibility and biocompatibility of solid polymeric materials and soluble targetable polymeric carrier. *Adv Drug Deliv Rev* 21:157–176.
- Rodríguez, F. J., Ceballos, D., Schüttler, M., Valderrama, E., Stieglitz, T. and Navarro, X. (2000). Polyimide cuff electrodes for peripheral nerve stimulation. *J Neurosci Methods* 98:105–118.
- Stieglitz, T. (2004). Considerations on surface and structural biocompatibility as prerequisite for long-term stability of neural prostheses. *J Nanosci Nanotechnol* 4:496–503.
- Stroncek, J. D. and Monty Reichert W. (2008). Overview of wound healing in different tissue types. In ‘Indwelling Neural Implants: Strategies for Contending with the *In Vivo* Environment’, Reichert WM, editor. Boca Raton (FL): CRC Press, 2008.
- Vince, V., Thil, M. A., Veraart, C., Colin, I. M. and Delbeke, J. (2004). Biocompatibility of platinum-metallized silicone rubber: In vivo and in vitro evaluation. *J Biomater Sci Polym* 15:173–188.
- Williams, D. F. (1987). Definitions in biomaterials. *Progress in Biomedical Engineering* 4: 54. Elsevier Science: Amsterdam.
- Williams, G. T. and Williams, W. J. (1983). Granulomatous inflammation – A review. *J Clin Pathol* 36:723–773.



